The fabrication and characterization of adjustable nanogaps between gold electrodes on chip for electrical measurement of single molecules

2010 Nanotechnology 21 274012

(http://iopscience.iop.org/0957-4484/21/27/274012)

Nanotechnology **21** (2010) 274012 (6pp) doi:10.1088/0957-4484/21/27/274012

The fabrication and characterization of adjustable nanogaps between gold electrodes on chip for electrical measurement of single molecules

Jing-Hua Tian[1,2], Yang Yang[1], Bo Liu[1], Bernd Schöllhorn[2], De-Yin Wu[1], Emmanuel Maisonhaute[2], Anna Serra Muns[2], Yong Chen[2], Christian Amatore[2], Nong-Jian Tao[3] and Zhong-Qun Tian[1]

[1] State Key Laboratory of Physical Chemistry of Solid Surfaces and LIA CNRS XiamENS 'NanoBioChem', College of Chemistry and Chemical Engineering, Xiamen University, Xiamen 361005, Fujian, People's Republic of China
[2] UMR CNRS 8640 'PASTEUR' and LIA CNRS XiamENS 'NanoBioChem', Ecole Normale Supérieure, Université Pierre et Marie Curie-Paris 6, 24 rue Lhomond, 75231 Paris Cedex 05, France
[3] Ira A Fulton School of Engineering and Center for Bioelectronics and Biosensors, Biodesign Institute, Arizona State University, Tempe, AZ 85287-6206, USA

E-mail: zqtian@xmu.edu.cn and christian.amatore@ens.fr

Received 28 November 2009, in final form 1 March 2010
Published 22 June 2010
Online at stacks.iop.org/Nano/21/274012

Abstract
This work reports on a new method to fabricate mechanically controllable break junctions (MCBJ) with finely adjustable nanogaps between two gold electrodes on solid state chips for characterizing electron transport properties of single molecules. The simple, low cost, robust and reproducible fabrication method combines conventional photolithography, chemical etching and electrodeposition to produce suspended electrodes separated with nanogaps. The MCBJ devices fabricated by the method can undergo many cycles in which the nanogap width can be precisely and repeatedly varied from zero to several nanometers. The method improves the success rate of the MCBJ experiments. Using these devices the electron transport properties of a typical molecular system, commercially available benzene-1,4-dithiol (BDT), have been studied. The I–V and G–V characteristic curves of BDT and the conductance value for a single BDT molecule established the excellent device suitability for molecular electronics research.

(Some figures in this article are in colour only in the electronic version)

1. Introduction

Molecular electronic devices have been attracting increasing attention in recent years because their many unique properties and functions [1–8]. However, large scale applications of molecular electronic devices are still hampered by two important technical difficulties. Firstly, there is no reliable method to fabricate electrodes separated with nanogaps for molecular junctions [9–16]. Secondly, one cannot yet predict reliably the electrical properties of molecular junctions based on the chemical structure of the molecules and the chemical bonds between the molecules and the electrodes [17–23].

Many methods have been proposed and developed to fabricate electrodes separated with gaps that are small enough to fit single molecules. Examples include electromigration, electrodeposition and etching based methods. Molecules with proper anchoring groups, such as thiol and pyridine, have been used to bridge the gaps between the electrodes to form molecular junctions [24–31]. However, despite successful examples, these methods have low fabrication yield, due to the

difficulty of reproducibly fabricating a gap with well-defined geometry and size. Studies have shown that the geometry of gold electrodes may evolve over time due to the high mobility of gold atoms on the surfaces [32]. Furthermore, the gaps between two electrodes fabricated with these methods cannot be flexibly adjusted after fabrication to fit molecules with different sizes.

Another widely used method for the formation and investigation of molecular junctions relies on scanning probe microscopy (SPM)-based break junctions, including scanning tunneling microscopy (STM) and conducting atomic force microscopy (c-AFM) [13, 33]. These methods allow for quick formation of molecular junctions by repeatedly moving the scanning tip in and out of contact with the substrate electrode in the presence of molecules. The conductances of a wide range of different molecules have then been determined on a statistical basis [34]. Besides the need for sophisticated instrumentation and delicate procedures, the statistical analysis based on transient measurements is not practical for device application. The mechanically controllable break junction (MCBJ) is a good approach that provides both flexibility and stability [35]. The gap between two electrodes can be controlled over a wide range with a precision below 1 Å while maintaining excellent stability [10, 11, 36, 37]. The MCBJ approach amounts to breaking a metal wire, by mechanically deforming an elastic substrate on which the wire is fixed, to create two electrodes with fresh and clean surfaces. By adjusting the mechanical deformation, the gap can be widened or closed continuously to fit different molecules. By opening and closing the gap repeatedly, one can fabricate a large number of molecular junctions and construct a histogram for reliable measurement of a single molecule conductance [12]. In general, the molecular junctions created with the MCBJ method are much more stable than those fabricated with the STM-based method. Finally, the MCBJ method allows fabrication of molecular junctions on silicon chips.

For the reasons discussed above, MCBJ has been widely used to investigate the electronic properties of single molecules [12, 34, 38–41]. The most popular methods to fabricate MCBJ devices use e-beam lithography and chemical etching of Si⟨100⟩ [42] or dry etching of sacrificial layers [43]. However, e-beam lithography is expensive and time-consuming, making it difficult for wide application. We report here on a simple, low cost and reliable approach to fabricate MCBJ devices and applications. Our method relies on a combination of conventional optical lithography, chemical etching and electrodeposition [44, 45]. The first stage of the method involves the creation of two electrodes separated by a micron-scale gap on a silicon wafer. This assembly is then suspended locally by chemical etching of an underlying micrometric silicon oxide layer initially deposited on the substrate. Finally, the gap distance between the electrode pair is reduced down to several angstroms evenly contacted by controlled electrodeposition. Using this method, we have been able to study electron transport in benzene-1,4-dithiol (BDT) and obtained the typically I–V and G–V characteristic curves of the BDT molecule and the conductance value of a single BDT molecule.

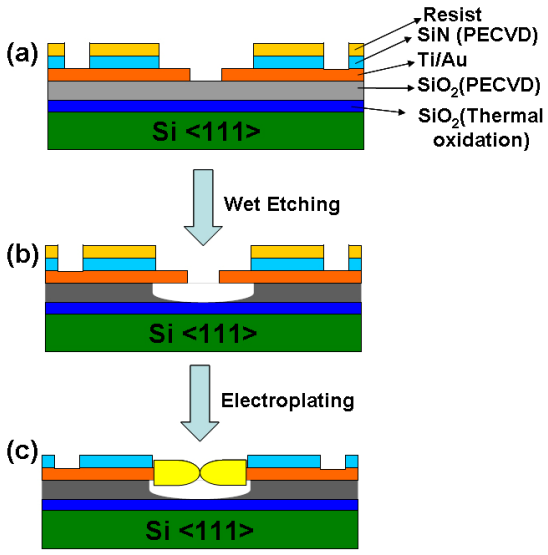

Figure 1. Schematic diagrams of the architecture of a MCBJ device before (a) and after (b) chemical etching of the PECVD SiO_2 layer and (c) electroplating (see text).

2. Experimental section

Optical lithography was used to fabricate electrode pairs (20 nm Ti/300 nm Au) on a 2.05 μm thick sacrificial SiO_2 layer deposited by plasma-enhanced chemical vapor deposition (PECVD) onto a silicon wafer initially covered by a 500 nm thick SiO_2 layer. The two electrodes in each pair were separated by about 2 μm. The electrodes were covered by a 400 nm thick Si_3N_4 layer, which was then selectively etched by reactive ion etching (RIE) and finally protected by depositing a layer of BP212 positive post-baked resist (figure 1(a)). Both layers were deposited and aligned so as to expose a portion of the electrode and bonding pads. The chip was then etched in 3 ml HF (40%):6 g NH_4F (40%):10 ml H_2O to remove the unprotected sacrificial PECVD-SiO_2 layer underneath the electrode pairs and create suspended electrodes (figure 1(b)).

The photoresist was then removed and the exposed electrodes were washed thoroughly with Milli-Q water before the electroplating stage. The principle of reducing the electrode gap width by gold electroplating from a 10 mM $Na_3Au(SO_3)_2$ + 50 mM $Na_2S_2O_3$ + 0.3 M $C_6H_8O_7$ (pH = 3–4) solution has been described in detail by us previously [44, 45]. Briefly, a three electrode system was used, using the galvanostatic mode with one of the electrodes in each pair on the silicon chip connected as the working electrode (WE) and an external gold wire used as the counter electrode (CE). The other electrode in the pair was left as a floating reference electrode (REF) so it did not experience any metal plating and its potential (V_{gap}) versus WE was monitored continuously during the electrodeposition process. Note that the roles of WE and REF can be exchanged during the electrodeposition process. Therefore, each of the paired electrodes could be gold plated with similar thicknesses. When the electrical double layer of the growing WE overlapped with the double layer of the REF electrode, V_{gap} decreased and

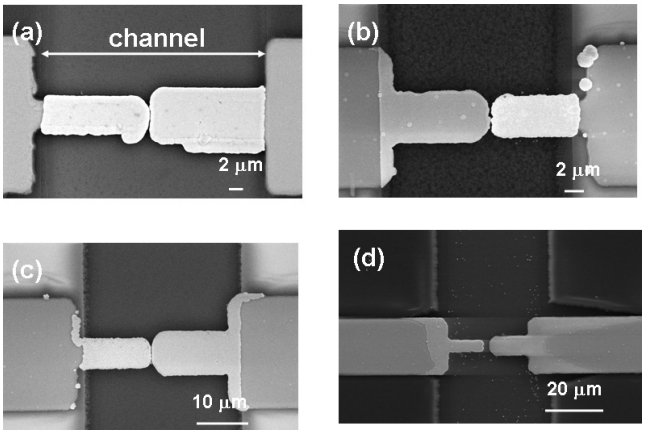

Figure 2. SEM images of electrode pairs after the PECVD SiO_2 unprotected layer was etched in 3 ml HF (40%):6 g NH_4F (40%):10 ml H_2O with different times: (a) 0 min; (b) 2 min; (c) 4 min; (d) 10 min. The channel width was 30 μm. Note in (d) that the presence of deterioration of the SiO_2 layer along the unrestricted sections of the electrodes was due to a too drastic etching duration.

eventually approached zero. By measuring V_{gap}, one can thus monitor the gap between the two electrodes. The resistance between the electrodes, measured with a semiconductor characterization system Keithley 4200, when V_{gap} dropped to zero was found to be smaller than 12.9 kΩ, the resistance quantum, indicating the formation of a quantum point contact between the two electrodes. However, when the electroplating process was dropped at different stages before $V_{gap} = 0$, the two electrodes were found to be separated with a nanometer- or angstrom-scale gap.

Figure 2 shows SEM images of several electrode pairs prepared with different wet etching times. Figure 2(b) is the SEM image of one electrode pair after 2 min wet etching, followed by electroplating and rinsing with Milli-Q water. The electroplating process resulted in a smooth and compact gold layer without affecting the Si_3N_4 insulation layer. However, compared to the chip without wet etching (see in figure 2(a)), the wet etching did cause surface roughening. The PECVD Si_3N_4 layer remains intact after the wet etching process because of the protection of the resist layer. The gold electrodes underneath the Si_3N_4 layer were also found to be intact after etching. Figure 2(c) shows an electrode pair after 4 min wet etching. It is clear that the electrodes are suspended from the substrate. Figure 2(d) is an SEM image of an electrode pair after 10 min wet etching. It clearly shows overetching that causes the electrodes to collapse. The optimal wet etching time was found to be 5–6 min, which allowed us to reproducibly fabricate suspended electrodes separated with a molecular scale gap or quantum point contact.

Figure 3(a) shows a close view of a connected electrode pair formed after waiting for V_{gap} to reach zero. The chip (figure 3(b)) was washed thoroughly with Milli-Q water and then mounted on a homemade MCBJ three-point force system constructed according to the procedure described previously [42, 43]. The separation between the electrodes was controlled by pushing the middle point of the system with either a piezoelectric or step motor drive (figure 3(c)). This

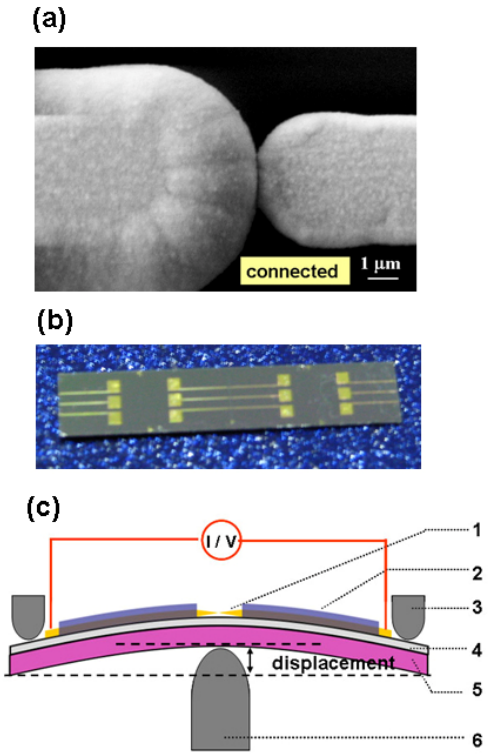

Figure 3. (a) SEM image of a pair of connected electrodes after electroplating; (b) photograph of a chip for MCBJ experiments; (c) schematic diagram of the MCBJ system developed in this work. 1: metal electrode pair; 2: insulating overlayer; 3: counter supports; 4: insulating layer; 5: bending beam; and 6: piezo or step motor driven pivot.

method allows flexible adjustment of the gap width with a sub-angstrom resolution (see section 3).

Molecular junctions were then formed by depositing a droplet of solution containing the sample molecules (BDT, 97%, AR, bought from Alfa Aesar, 0.1 mM in ethanol) [10, 11]. Initially the gap width was set up at 2–3 nm, and it was then reduced continuously while monitoring the current between the electrode pair with the Keithley 4200. The bias voltage between the two electrodes during the experiment was maintained at 100 mV. The appearance of a current plateau indicated the formation of a molecular junction [11, 38]. The gap was then fixed to allow the recording of current–voltage (I–V) characteristic curves between -1 and $+1$ V. The conductance–voltage (G–V) curves were obtained by taking numerical derivatives of the I–V curves. An alternative procedure used here was to continuously sweep the bias voltage under different gap sizes when slowly closing the gap.

3. Results and discussion

3.1. Fabrication of suspended electrodes separated with controlled gaps

The optical lithography procedure, described in section 2, allowed us to fabricate a pair of electrodes pointing to each other with a gap of $\sim$2 μm on a 2.05 μm silicon oxide layer that served as a sacrificial layer (figure 1(a)). The

electrodes were protected by a Si_3N_4 layer and then by a photoresist, except for the gap region for wet etching and electroplating, and the bonding pads for electrical connection. The silicon oxide sacrificial layer underneath the electrodes was etched to suspend the electrodes (figure 1(b)). After thorough washing, the gap between the two electrodes was reduced by electroplating gold onto each of the two electrodes sequentially [44, 45]. The final gap was reduced below 1 nm, as required for the formation of a molecular junction (figures 2 and 3). To achieve such a small gap, the electroplating process was carefully monitored by measuring the potential difference, V_{gap}, between the electrode under electroplating (serving as working electrodes or WE) and the second electrode (serving as reference electrode or RE). When the electrical double layers of the two electrodes began to overlap with each other, V_{gap} decreased continuously, and eventually approached zero when the two electrodes formed a quantum point contact. So the value of V_{gap} provides a good indicator of the gap width. The gap width could be controlled by stopping the electroplating process at an appropriate V_{gap}.

After the electroplating procedure, the chips were thoroughly rinsed with water and dried with a nitrogen gas flow. The measurement of the resistance or the conductance between the two electrodes allowed us to detect point contacts between the two electrodes. If the conductance was greater than a unit quantum conductance, $G_0 = 2e^2/h = 77.5\ \mu$S, a point contact was formed. A smaller value of G indicated that the two electrodes remained separated [39, 46]. The determination of the gap width (g) was based on the tunneling current, I_t.

$$I_t = G_0 \Delta V \exp(-kg) \tag{1}$$

where ΔV is the applied bias voltage across the gap and k the tunneling decay constant. The particularly high precision of the MCBJ technique is due to the exponential dependence of the tunneling current on the gap size.

We point out that the electroplating method is simple and low cost in comparison with the electron beam lithography commonly used to fabricate MCBJ on solid chips. A typical conductance curve recorded during the breakdown of a pair of electrodes is shown in figure 4. The well-defined plateaus are well known for quantum point contact [37]. After breaking the last atomic contact, the current decays exponentially, as expected for a tunneling process. Since the rate for opening the gap is slow, it appears more clearly compared to other methods such as a STM-break junction [13], and the conductance does not drop to zero immediately.

One advantage of MCBJ is that the gap can be opened immediately before adsorption of the molecular probe to be studied, which minimizes contamination of the electrodes. Weakly adsorbed material would nevertheless be removed by the strongly binding thiols studied in this paper.

After breaking the quantum point contact, the gap between the two electrodes was controlled with the setup shown in figure 3(c) [42, 43]. The relative displacement $r = \Delta g/\Delta z$ of the two electrodes separation displacement (Δg) versus the upward movement of the central point (Δz) is given by [43]

$$r = 6t_S u/l^2 \tag{2}$$

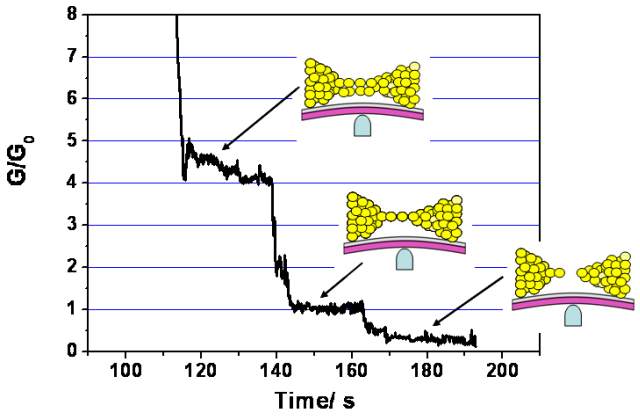

Figure 4. Typical recording of the conductance G measured in the opening process of a gold electrode pair with MCBJ when the central pivot was moved upward at a constant displacement rate. The applied potential bias was 100 mV.

where t_S is the thickness of the substrate, u the total length of the suspended portions of the electrodes, and l the separation of the two counter supports. If $u = 0$, then $r = 0$, which means that the gap width could not be changed much if the electrodes were not suspended. The suspension of the electrodes allowed us to control the gap continuously and also drastically improved the success rate of the MCBJ experiments. The success rate was high also because of the electroplating that brought the two electrodes close to each other so that only a relatively small amount of mechanical actuation (bending) was required to tune the gap width for fitting single molecules.

The thickness of the substrate used in our MCBJ was $t_S = 300\ \mu$m and the separation of the two counter supports was $l = 20$ mm. The length of the suspended electrodes, u, could be varied, but a typical value of $\sim$30 μm was used. Using these parameters, equation (2) predicts that $r \approx 1.35 \times 10^{-4}$. In other words, if the central pivot moves upward by $\Delta z = 1\ \mu$m, the gap width increases by $\Delta g = 1.35$ Å. This demagnification is critical for the high precision and stability of MCBJ. r can be even further decreased upon reducing u.

Figure 5 shows an example for $u = 2\ \mu$m. It plots both the gap width determined from the tunneling current, and the displacement of the central pivotal point. Several conclusions can be drawn from the data. First, it shows a linear dependence of the gap width on the upward and downward movements of the central pivot point. Second, the plot demonstrates that the gap width can be reproducibly controlled by repeatedly moving the pivot point up and down. Third, it demonstrates high stability. Fourth, from figure 5, we determined that $r = 0.1$ Å μm^{-1} which is in good agreement with the prediction of equation (2). Finally the gap width was not influenced by mechanical and acoustic noises [47]. All these results are very similar and coincident with [42].

3.2. Investigation of molecular junctions

Measurements of the molecular conductance of BDT, the model molecule in molecular electronics, were performed

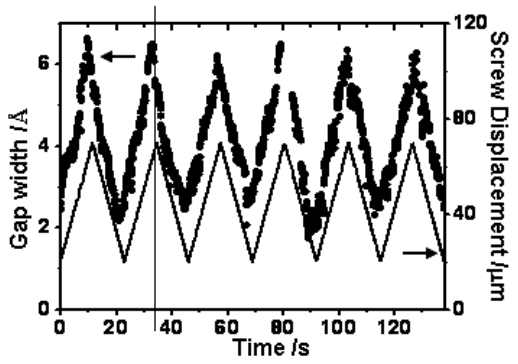

Figure 5. Correlation between gap width (dotted curve) and cyclic linear displacement of the central pivot (solid curve). $t = 300$ μm, $l = 20$ mm and $u = 2$ μm.

using the MCBJ described above. The molecular conductance of BDT has been well established already [10, 38, 48, 49]. At the beginning of each experiment, the gap width was maintained at 2–3 nm, as estimated from the tunneling current (or tunneling resistance of 10^{11}–10^{12} Ω). A droplet of 0.1 mM BDT in ethanol was then placed over the junction to allow molecules to adsorb and bridge the gap across the electrodes [10, 11]. The gap was then closed gradually while the current flowing through the electrode pair at a potential bias of 100 mV was monitored continuously. Once a molecule bridged between the two electrodes, which was indicated by the occurrence of a steady current plateau [11, 39], the gap width was frozen and the I–V characteristics of the molecular junction was determined by sweeping the applied bias voltage. For all the electrical measurements the MCBJ was introduced inside a bronze Faraday cage to eliminate electromagnetic noise.

Figure 6 shows an example of typical I–V characteristics (black curve) together with the corresponding conductance-potential G–V (blue curve) of a Au/BDT/Au junction under different voltages ranges. For a small bias range, the I–V curves are linear (figure 6(a)), the conductance was found to be 49 ± 0.8 nS from the slope of the linear regime, which is in agreement with that of the previous report [10]. Increasing the bias range to above +0.2 V and below −0.2 V (figure 6(b)), the current increased to several tens of nanoamperes (nA), and the I–V curve began to deviate from simple linear behavior, but still had symmetric behavior. When the voltages was increased above +0.5 V or below −0.5 V continuously (figure 6(c)), the current increased dramatically, up to microamperes, and the curve deviated considerably from linear behavior, but still remained almost symmetric; as predicted theoretically for a symmetrical molecule [50].

4. Conclusions

We have demonstrated a successful combination of conventional photolithography, chemical etching and electroplating to fabricate suspended electrode pairs suitable for MCBJ applications. The simplicity, reproducibility and robustness of the fabrication method makes it useful for studying the electron transport properties of molecular junctions. Using this method, we have fabricated MCBJ, characterized their stability, linearity and reproducibility, and calibrated the adjustable gap width. Electron transport in a typical model molecule, BDT, was studied in detail. The MCBJ devices fabricated with the present method could be particularly suitable for studying electron transport via molecules in an electrochemical environment [51] and also for surface-enhanced Raman spectroscopy [52, 53]; these are currently being studied in our laboratory.

Acknowledgments

This work was supported in part by NSF (Grant 20620130427) and MOST (Grants 2007DFC40440, 2009CB930703) in China, Open Project of State Key Laboratory of Supramolecular Structure and Materials (SKLSSM200701), Jilin Univ., China, and by CNRS (UMR 8640 'PASTEUR'), Ecole Normale Supérieure (ENS), University Pierre and Marie Curie (UPMC), French Ministry of Research in France through ANR REEL, and by US-NSF (DMR-03-05242).

References

[1] Carroll R L and Gorman Christopher B 2002 *Angew. Chem. Int. Edn Engl.* **41** 4378–400
[2] Nitzan A and Ratner M A 2003 *Science* **300** 1384–9

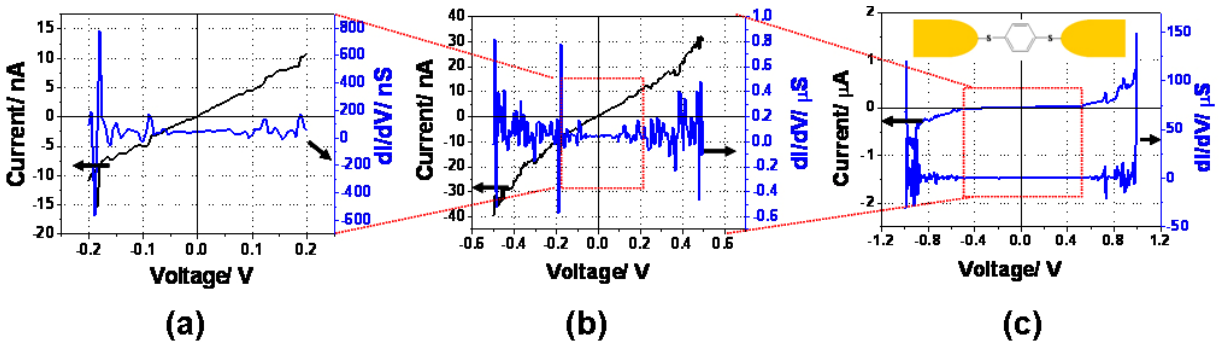

Figure 6. Successive zoom out graphs of measured I–V and G–V curves of an Au/BDT/Au molecular junction under different voltage sweep ranges (a) −0.2–+0.2 V; (b) −0.5–+0.5 V and (c) −1.0–+1.0 V. Inset of (c) is a schematic drawing of Au/BDT/Au structure.

[3] Chen F, Hihath J, Huang Z, Li X and Tao N J 2007 *Annu. Rev. Phys. Chem.* **58** 535–64
[4] Tao N J 2006 *Nat. Nanotechnol.* **1** 173–81
[5] Tour J M 2000 *Acc. Chem. Res.* **33** 791–804
[6] Mantooth B A and Weiss P S 2003 *Proc. IEEE* **91** 1785–802
[7] McCreery R L 2004 *Chem. Mater.* **16** 4477–96
[8] Ulgut B and Abruna H D 2008 *Chem. Rev.* **108** 2721–36
[9] Cui X D, Primak A, Zarate X, Tomfohr J, Sankey O F, Moore A L, Moore T A, Gust D, Harris G and Lindsay S M 2001 *Science* **294** 571–4
[10] Reed M A, Zhou C, Muller C J, Burgin T P and Tour J M 1997 *Science* **278** 252–4
[11] Reichert J, Ochs R, Beckmann D, Weber H B, Mayor M and von Lohneysen H 2002 *Phys. Rev. Lett.* **88** 176804
[12] Gonzalez M T, Wu S, Huber R, van der Molen S J, Schoenenberger C and Calame M 2006 *Nano Lett.* **6** 2238–42
[13] Xu B and Tao N J 2003 *Science* **301** 1221–3
[14] Haiss W, Nichols R J, van Zalinge H, Higgins S J, Bethell D and Schiffrin D J 2004 *Phys. Chem. Chem. Phys.* **6** 4330–7
[15] Yasuda S, Yoshida S, Sasaki J, Okutsu Y, Nakamura T, Taninaka A, Takeuchi O and Shigekawa H 2006 *J. Am. Chem. Soc.* **128** 7746–7
[16] Donhauser Z J *et al* 2001 *Science* **292** 2303–7
[17] Galperin M, Ratner M A and Nitzan A 2004 *Nano Lett.* **4** 1605–11
[18] Wang W, Lee T, Kretzschmar I and Reed M A 2004 *Nano Lett.* **4** 643–6
[19] Jun Y and Zhu X Y 2004 *J. Am. Chem. Soc.* **126** 13224–5
[20] Jaiswal A, Tavakoli K G and Zou S 2006 *Anal. Chem.* **78** 120–4
[21] Nowak A M and McCreery R L 2004 *J. Am. Chem. Soc.* **126** 16621–31
[22] McCreery R L 2006 *Anal. Chem.* **78** 3490–7
[23] Ward D R, Halas N J, Ciszek J W, Tour J M, Wu Y, Nordlander P and Natelson D 2008 *Nano Lett.* **8** 919–24
[24] Morpurgo A F, Marcus C M and Robinson D B 1999 *Appl. Phys. Lett.* **74** 2084–6
[25] Park H, Lim A K L, Alivisatos A P, Park J and McEuen P L 1999 *Appl. Phys. Lett.* **75** 301–3
[26] Mahapatro Ajit K and Janes David B 2007 *J. Nanosci. Nanotechnol.* **7** 2134–8
[27] Strachan D R, Smith D E, Johnston D E, Park T H, Therien M J, Bonnell D A and Johnson A T 2005 *Appl. Phys. Lett.* **86** 043109
[28] Johnston D E, Strachan D R and Johnson A T C 2007 *Nano Lett.* **7** 2774–7
[29] Yu L H and Natelson D 2004 *Nano Lett.* **4** 79–83
[30] Selzer Y, Cabassi Marco A, Mayer Theresa S and Allara David L 2004 *J. Am. Chem. Soc.* **126** 4052–3
[31] Li C Z, He H X and Tao N J 2000 *Appl. Phys. Lett.* **77** 3995–7
[32] Sondag-Huethorst J A M, Schonenberger C and Fokkink L G J 1994 *J. Phys. Chem.* **98** 6826–34
[33] Xu B, Xiao X and Tao N J 2003 *J. Am. Chem. Soc.* **125** 16164–5
[34] van Ruitenbeek J, Scheer E and Weber H B 2005 *Lect. Notes Phys.* **680** 253–74
[35] Muller C J, van Ruitenbeek J M and de Jongh L J 1992 *Physica C* **191** 485–504
[36] Kang N, Erbe A and Scheer E 2008 *New J. Phys.* **10** 9
[37] Agrait N, Yeyati A L and van Ruitenbeek J M 2003 *Phys. Rep.* **377** 81–279
[38] Lortscher E, Weber H B and Riel H 2007 *Phys. Rev. Lett.* **98** 176807
[39] Lortscher E, Ciszek J W, Tour J and Riel H 2006 *Small* **2** 973–7
[40] Smit R H M, Noat Y, Untiedt C, Lang N D, van Hemert M C and van Ruitenbeek J M 2002 *Nature* **419** 906–9
[41] Huisman E H, Trouwborst M L, Bakker F L, de Boer B, van Wees B J and van der Molen S J 2008 *Nano Lett.* **8** 3381–5
[42] Zhou C, Muller C J, Deshpande M R, Sleight J W and Reed M A 1995 *Appl. Phys. Lett.* **67** 1160–2
[43] van Ruitenbeek J M, Alvarez A, Pineyro I, Grahmann C, Joyez P, Devoret M H, Esteve D and Urbina C 1996 *Rev. Sci. Instrum.* **67** 108–11
[44] Xiang J, Liu B, Wu S-T, Ren B, Yang F-Z, Mao B-W, Chow Y L and Tian Z-Q 2005 *Angew. Chem. Int. Edn Engl.* **44** 1265–8
[45] Liu B, Xiang J, Tian J-H, Zhong C, Mao B-W, Yang F-Z, Chen Z-B, Wu S-T and Tian Z-Q 2005 *Electrochim. Acta* **50** 3041–7
[46] Yanson A I, Bollinger G R, van den Brom H E, Agrait N and van Ruitenbeek J M 1998 *Nature* **395** 783–5
[47] Muller C J and de Bruyn Ouboter R 1995 *J. Appl. Phys.* **77** 5231–6
[48] Horiguchi K, Tsutsui M, Kurokawa S and Sakai A 2009 *Nanotechnology* **20** 025204
[49] Xiao X, Xu B and Tao N J 2004 *Nano Lett.* **4** 267–71
[50] Jiang J, Kula M and Luo Y 2006 *J. Chem. Phys.* **124** 034708
[51] Xiao X, Brune D, He J, Lindsay S, Gorman C B and Tao N 2006 *Chem. Phys.* **326** 138–43
[52] Kneipp K, Wang Y, Kneipp H, Perelman L T, Itzkan I, Dasari R R and Feld M S 1997 *Phys. Rev. Lett.* **78** 1667–70
[53] Nie S and Emory S R 1997 *Science* **275** 1102–6